Canted antiferromagnetic phase of the $\nu = 0$ quantum Hall state in bilayer graphene

Maxim Kharitonov Center for Materials Theory, Rutgers University, Piscataway, NJ 08854, USA (Dated: October 30, 2018)

Motivated to understand the nature of the strongly insulating $\nu=0$ quantum Hall state in bilayer graphene, we develop the theory of the state in the framework of quantum Hall ferromagnetism. The generic phase diagram, obtained in the presence of the isospin anisotropy, perpendicular electric field, and Zeeman effect, consists of the spin-polarized ferromagnetic (F), canted antiferromagnetic (CAF), and partially (PLP) and fully (FLP) layer-polarized phases. We address the edge transport properties of the phases. Comparing our findings with the recent data on suspended dual-gated devices, we conclude that the insulating $\nu=0$ state realized in bilayer graphene at lower electric field is the CAF phase. We also predict a continuous and a sharp insulator-metal phase transition upon tilting the magnetic field from the insulating CAF and FLP phases, respectively, to the F phase with metallic edge conductance $2e^2/h$, which could be within the reach of available fields and could allow one to identify and distinguish the phases experimentally.

PACS numbers: 73.43.-f, 71.10.Pm, 73.43.Lp

Introduction. One of the most intriguing questions in today's graphene research concerns the nature of the strongly insulating $\nu = 0$ quantum Hall (QH) state [with half-filled zero-energy Landau level ($\epsilon = 0 \text{ LL}$)], observed in both monolayer (MLG) [1] and bilayer (BLG) [2-6] graphene with two-terminal conductance of the highest quality samples $G \lesssim 10^{-5}e^2/h$. While the basic theoretical framework of the interaction-induced $\nu = 0$ state – the concept of generalized quantum Hall ferromagnetism (QHFMism) [7] – is well-established [8–17], it is unambiguously identifying the particular order of the $\nu = 0$ QHFM that presents a challenge. Given the rich phase diagram of the $\nu = 0$ QHFM in MLG [10–13] (and as we show here, in BLG) and the fact that all phases but the spin-polarized one [18, 19] are expected to be fully insulating [11, 20, 21], achieving this goal requires a more detailed both theoretical and experimental analysis.

On the experimental side, in BLG, a crucial step in this direction was recently made in dual-gated suspended devices [4, 6], where application of perpendicular electric field E offers a unique possibility to ma-

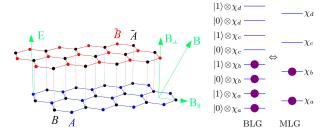


FIG. 1: (color online). (left) Lattice structure of BLG. (right) Occupation of the $01 \otimes KK' \otimes s$ space of each orbital by four electrons in the $\nu=0$ QHFM state in BLG. The energy of the $KK' \otimes s$ -symmetric interactions is minimized by forming 01-pseudospin-singlet pairs [14, 15]. Correspondence between the $\nu=0$ QHFM states in BLG and MLG is shown.

nipulate the layer "isospin". At perpendicular magnetic fields $B_{\perp} \gtrsim 1 \mathrm{T}$, upon applying the electric field, a phase transition to yet another insulating QH state with $G \ll e^2/h$ was observed, which can be readily identified as the valley=layer-polarized phase of the $\nu=0$ QHFM. This transition was characterized by a spike in conductance with maximum $G \sim e^2/h$ at the critical field $E^* \approx 11 B_{\perp} [\mathrm{T}] \mathrm{meV/nm}$ and was observed for both polarities of the electric field.

Motivated by this result, in this Letter we develop the theory of the $\nu=0$ QHFM in BLG. We obtain a generic phase diagram in the presence of the isospin anisotropy of electron-electron (e-e) [10, 11, 13] and electron-phonon (e-ph) [12, 13] interactions, electric field, and Zeeman effect. We address the edge transport properties of the phases. Comparing our findings with the data of Refs. 4, 6, we arrive at the conclusion that the insulating $\nu=0$ QH state realized in BLG at lower electric field [2–6] is the canted antiferromagnetic phase of the $\nu=0$ QHFM: the very existence of the phase transitions with applied electric field provides sufficient information for that. We also predict that experiments in the tilted magnetic field could verify this conclusion and allow for observation of new phase transitions.

 $\nu=0$ QHFM in BLG. Our analysis follows closely that for MLG [13], and details will be presented elsewhere [21]. The $\epsilon=0$ LL in BLG, located at the charge neutrality point, possesses very peculiar properties [22]. First, analogous to the case in MLG, in each valley, K or K', its wave functions reside on only one sublattice, \tilde{B} or A, of the low-energy two-band model [22] and hence in either one of the layers (Fig. 1). This makes not only the $A\tilde{B}$ sublattice and layer, but also the valley degree of freedom equivalent, $K \leftrightarrow \tilde{B}$, $K' \leftrightarrow A$ (referred to as KK' "isospin" here). Second, both $|0\rangle$ and $|1\rangle$ magnetic oscillator states belong to the $\epsilon=0$ LL, which results in its unique extra twofold orbital degeneracy (this subspace is referred to as 01 "pseudospin" here). Each orbital of the

 $\epsilon = 0$ LL is thus (approximately) eightfold degenerate in the $01 \otimes KK' \otimes s$ pseudospin-isospin-spin space.

According to the general theory of QHFMism [7], at integer filling factors ν , Coulomb interactions result in spontaneous ordering of discrete degrees of freedom (spin, valley, etc), favoring the many-body states, in which each orbital is occupied by electrons in exactly the same way. At the $\epsilon = 0$ LL in BLG, due to the difference in wave functions of the $|0\rangle$ and $|1\rangle$ states, interactions possess an intrinsic anisotropy in the 01-pseudospin space [14, 15]. As demonstrated in Refs. [14, 15], at $\nu = 0$ the energy minimum of the $KK' \otimes s$ -symmetric interactions is delivered by those QHFM states, in which four electrons per orbital occupy the states $|0\rangle \otimes \chi_a$, $|1\rangle \otimes \chi_a$, $|0\rangle \otimes \chi_b$, $|1\rangle \otimes \chi_b$ with arbitrary orthogonal spinors $\chi_{a,b}$ in the $KK' \otimes s$ space, i.e., form two pseudospin-singlet pairs (Fig. 1). Ordering of the remaining isospin-spin degrees of freedom is governed by (weaker) mechanisms of the $KK' \otimes s$ -symmetry breaking. Following Ref. [13], the energy (per orbital per electron in a pair)

$$\mathcal{E}(P) = \mathcal{E}_{\diamond}(P) + \mathcal{E}_{V}(P) + \mathcal{E}_{Z}(P), \tag{1}$$

$$\mathcal{E}_{\diamond}(P) = \frac{1}{2} \sum_{\alpha} u_{\alpha} \{ \operatorname{tr}^{2}[\mathcal{T}_{\alpha}P] - \operatorname{tr}[\mathcal{T}_{\alpha}P\mathcal{T}_{\alpha}P] \}, \quad (2)$$

$$\mathcal{E}_V(P) = -\epsilon_V \operatorname{tr}[\mathcal{T}_z P], \ \mathcal{E}_Z(P) = -\epsilon_Z \operatorname{tr}[S_z P], \ \ (3)$$

of these effects as a function of the order parameter matrix $P = \chi_a \chi_a^{\dagger} + \chi_b \chi_b^{\dagger}$ is obtained by calculating the expectation value of the microscopic Hamiltonian for BLG with respect to the family of QHFM states. Here, $\alpha=x,y,z,~\mathcal{T}_{\alpha}=\tau_{\alpha}^{KK'}\otimes\hat{1}^{s},~S_{z}=\hat{1}^{KK'}\otimes\tau_{z}^{s},~\tau_{\alpha}$ are the Pauli matrices, and tr[...] is the matrix trace. The singleparticle electric field $[\mathcal{E}_V(P)]$ and Zeeman $[\mathcal{E}_Z(P)]$ effects are characterized by the energies $\epsilon_V \approx E a_z/2$ [23], where $a_z \approx 3.5 \text{Å}$ is the interlayer distance, and $\epsilon_Z = \mu_B B$, where $B = \sqrt{B_{\perp}^2 + B_{\parallel}^2}$ is the total magnetic field. The magnetic field B has arbitrary direction relative to the sample (Fig. 1) and the z axis in spin space is chosen along it. The many-body KK'-symmetry-breaking effects of e-e and e-ph interactions, crucial in determining the preferred ground-state order, give rise to the isospin anisotropy $\mathcal{E}_{\diamond}(P)$. Its generic form (2) is fully characterized by two signed B_{\perp} -dependent energies $u_{\perp} \equiv$ $u_x = u_y$ and u_z . The bare energies can roughly be estimated [10, 12] as $|u_{\perp,z}^{(0)}| \sim e^2 a/l_B^2 \sim 1 - 10 B_{\perp}[T] K$, where a is some lattice spatial scale and $l_B = \sqrt{\hbar c/(eB_\perp)}$, and can be further renormalized [13].

Phase diagram. The zero-temperature mean-field phase diagram is obtained by minimizing the energy $\mathcal{E}(P)$ [24]. Remarkably, the theory of the $\nu=0$ QHFM in BLG described by Eqs. (1), (2), and (3) appears to be formally equivalent to that in MLG [13], upon identifying the pseudospin-singlet electron pairs in BLG with single electrons in MLG (Fig. 1): $\{|0\rangle, |1\rangle\} \otimes \chi_{a,b} \leftrightarrow \chi_{a,b}$.

In particular, the phase diagram at zero electric field, $\epsilon_V = 0$, is identical to that in MLG [13]. The anisotropy

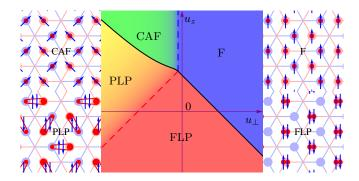


FIG. 2: (color online). Phase diagram of the $\nu=0$ QHFM in BLG in the space of isospin anisotropy energies (u_{\perp}, u_z) at fixed electric ϵ_V and Zeeman ϵ_Z energies.

energy $\mathcal{E}_{\diamond}(P)$ alone is minimized by one of the following phases (Fig. 16 in Ref. [13]): spin-polarized isospinsinglet ferromagnetic (F, $\chi_a = |K\rangle \otimes |\mathbf{s}\rangle$, $\chi_b = |K'\rangle \otimes |\mathbf{s}\rangle$) at $u_{\perp} > 0$, $u_{\perp} + u_{z} > 0$; antiferromagnetic (AF, $\chi_a = |K\rangle \otimes |\mathbf{s}\rangle, \ \chi_b = |K'\rangle \otimes |-\mathbf{s}\rangle, \ \text{with antiparal-}$ lel spin polarizations $\pm \mathbf{s}$ of the layers, at $u_z > -u_{\perp} >$ 0; and two isospin-polarized spin-singlet phases: fully layer-polarized phase [FLP, $\chi_a = |\pm \mathbf{n}_z\rangle \otimes |\uparrow\rangle$, $\chi_b =$ $|\pm \mathbf{n}_z\rangle \otimes |\downarrow\rangle$, $\mathbf{n}_z = (0,0,1)$, analogue of the chargedensity-wave (CDW) phase in MLG at $-u_{\perp} > |u_z|$ and, in the terminology of QH bilayers [7], interlayercoherent phase [ILC, $\chi_a = |\mathbf{n}_{\perp}\rangle \otimes |\uparrow\rangle$, $\chi_b = |\mathbf{n}_{\perp}\rangle \otimes |\downarrow\rangle$, $\mathbf{n}_{\perp} = (\cos \varphi_n, \sin \varphi_n, 0)$, analogue of the Kekulé distortion (KD) phase in MLG] at $-u_z > |u_\perp|$. Here and below, \mathbf{s} and \mathbf{n} are the unit vectors defining the spin and isospin polarizations of the states $|\mathbf{s}\rangle$ and $|\mathbf{n}\rangle$, respectively; $\pm \mathbf{n}_z \leftrightarrow K, K'$ and $\pm \mathbf{s}_z \leftrightarrow \uparrow, \downarrow$. The F and AF phases are SU(2)-spin-degenerate (s), and the ILC and FLP phases are U(1)- and Z_2 -isospindegenerate $(\varphi_n \text{ and } \pm \mathbf{n}_z)$, respectively. Including the Zeeman effect [minimization of $\mathcal{E}_{\diamond}(P) + \mathcal{E}_{Z}(P)$, Fig. 18 in Ref. [13] does not affect the spin-singlet ILC and FLP phases but lifts the spin degeneracy of the F phase, $\mathbf{s} \rightarrow \mathbf{s}_z = (0,0,1)$, and transforms the AF phase to the U(1)-spin-degenerate (φ_s) canted antiferromagnetic phase (CAF, $\chi_a = |K\rangle \otimes |\mathbf{s}_a^*\rangle$, $\chi_b = |K'\rangle \otimes |\mathbf{s}_b^*\rangle$), in which the layers have noncollinear spin polarizations $\mathbf{s}_{a,b}^* = (\pm \sin \theta_s^* \cos \varphi_s, \pm \sin \theta_s^* \sin \varphi_s, \cos \theta_s^*)$ with the optimal projection $s_z^* = \cos \theta_s^* = \epsilon_Z/(2|u_\perp|)$ on the total magnetic field.

Including the effect of electric field [minimization of $\mathcal{E}(P)$] does not affect the F and CAF phases but lifts the isospin degeneracy of the FLP phase, $\pm \mathbf{n}_z \to \mathbf{n}_z$, and transforms the ILC phase to the partially layer-polarized phase (PLP, $\chi_a = |\mathbf{n}^*\rangle \otimes |\uparrow\rangle$, $\chi_b = |\mathbf{n}^*\rangle \otimes |\downarrow\rangle$), in which the valley=layer isospin $\mathbf{n}^* = (\sin\theta_n^*\cos\varphi_n, \sin\theta_n^*\sin\varphi_n, \cos\theta_n^*)$ has the optimal value $n_z^* = \cos\theta_n^* = \epsilon_V/(u_z + |u_\perp|)$ of the projection characterizing the degree of layer charge polarization. As a result, in the presence of generic isospin anisotropy, electric field,

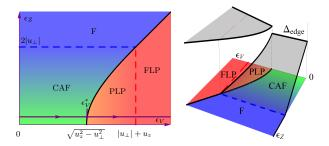


FIG. 3: (color online). (left) Phase diagram in the space (ϵ_V, ϵ_Z) of electric and Zeeman energies at fixed anisotropy energies $u_{\perp,z}$, for the case (5) of AF phase favored by the isospin anisotropy. The violet line denotes the evolution of the system with applied electric field, realized in Ref. [4, 6], with the CAF-PLP insulator-insulator transition at $\epsilon_V = \epsilon_V^*$ characterized by a conductance spike. (right) Qualitative behavior of the edge transport gap $\Delta_{\rm edge}$ as a function of ϵ_V and ϵ_Z . In the CAF phase, $\Delta_{\rm edge}$ gradually decreases upon tilting the magnetic field and closes completely once the F phase is reached.

and the Zeeman effect, the phase diagram of the $\nu=0$ QHFM in BLG consists of the F, CAF, PLP, and FLP phases (Fig. 2) with energies $\mathcal{E}^{\rm F}=-2u_{\perp}-u_z-2\epsilon_Z$, $\mathcal{E}^{\rm CAF}=-u_z-\epsilon_Z^2/(2|u_{\perp}|), \,\mathcal{E}^{\rm PLP}=u_{\perp}-\epsilon_V^2/(u_z+|u_{\perp}|),$ and $\mathcal{E}^{\rm FLP}=u_z-2\epsilon_V$. The phase boundaries, obtained by comparing the energies, are $u_z-u_{\perp}=\epsilon_V$ for PLP-FLP, $u_{\perp}=-\epsilon_Z/2$ for CAF-F, $u_z+u_{\perp}=\epsilon_V-\epsilon_Z$ for F-FLP, and

$$u_{\perp} + u_z = \epsilon_V^2 / (u_z - u_{\perp}) + \epsilon_Z^2 / (2u_{\perp})$$
 (4)

for CAF-PLP phase transitions, respectively.

In real BLG, the actual signs and ratio of $u_{\perp,z}(B_{\perp})$, which define the ground-state order at $\epsilon_V = \epsilon_Z = 0$, are determined by details of e-e and e-ph interactions at the lattice scale. Therefore, in practice, transitions between different phases can potentially be realized by varying the electric ϵ_V or Zeeman $\epsilon_Z = \mu_B B$ energies relative to the anisotropy energies $u_{\perp,z}(B_{\perp})$ (Fig. 3) where the latter is achieved by tilting the magnetic field.

Edge transport. Given the formal equivalence of the low-energy theories, one can expect the edge charge excitations of the $\nu=0$ QHFM in BLG and MLG to have qualitatively the same properties, despite the differences in microscopic structures [25] of the edges. Below we combine the earlier predictions for MLG [11, 18–20] with general physical arguments to arrive at the anticipated [21] edge transport phase diagram.

The charge of collective Skyrmion-type excitations of the $\nu=0$ QHFM in BLG, associated with inhomogeneous isospin-spin textures $P(\mathbf{r})$, is 2e-quantized [15] due to binding of electrons into pseudospin-singlet pairs. Since in MLG collective edge excitations of the F phase are gapless [19], we conclude that the F phase in BLG supports gapless collective 2e-charge edge excitations and an ideal sample has a metallic $2e^2/h$ conductance per

edge.

The AF and CDW phases in MLG are predicted to have gapped edge excitations [11, 20], which can be seen as special cases of a more general property. Noting that the isospin-singlet F phase is the only phase that does not break the valley symmetry, one can argue that, in fact, all other orders of the $\nu=0$ QHFM have gapped [26] edge excitations. In particular, the remaining CAF, PLP, and FLP phases are expected to be fully insulating (note that bulk charge excitations are gapped in any phase).

Further distinction between the insulating phases is made by noticing the following properties. The PLP $(0 < n_z^* < 1)$ and CAF $(0 < s_z^* < 1)$ phases continuously interpolate between their limiting cases, ILC $(n_z^* = 0)$, FLP $(n_z^* = 1)$ and AF $(s_z^* = 0)$, F $(s_z^* = 1)$ phases, which can be tuned by applying the electric field (ϵ_V) and tilting the magnetic field (ϵ_Z) , respectively. Therefore, CAF-F and PLP-FLP are continuous second-order (at zero temperature) phase transitions (dashed blue and red lines in Figs. 2 and 3) and no sudden changes in transport properties, such as a conductance spike, should occur there. Consequently, first, the system remains insulating as it transitions from the PLP to FLP phase, without a sharp feature of the PLP-FLP transition in transport. Second, since AF and F phases have gapped and gapless edge charge excitations, respectively, we are forced to conclude, by continuity, that the edge transport gap $\Delta_{\mathrm{edge}}^{\mathrm{CAF}}(s_z^*)$ of the CAF phase monotonically decreases with $s_z^* = \epsilon_Z/(2|u_\perp|)$ from a finite value $\Delta_{\mathrm{edge}}^{\mathrm{CAF}}(s_z^*=0) = \Delta_{\mathrm{edge}}^{\mathrm{AF}}$ at $\epsilon_Z=0$ to zero $\Delta_{\mathrm{edge}}^{\mathrm{CAF}}(s_z^*=1) = \Delta_{\mathrm{edge}}^{\mathrm{F}}=0$ at the CAF-F boundary $\epsilon_Z=2|u_\perp|$. I.e., the continuous transformation of the CAF to F phase upon tilting the field is accompanied by gradual closing of the edge transport gap. In contrast to the latter, the edge transport gap of the spin-singlet PLP and FLP phases is not expected to appreciably depend on ϵ_Z .

On the other hand, CAF-PLP and F-FLP are discontinuous first-order phase transitions (black solid lines in Figs. 2 and 3), which could be signified by conductance spikes due to increased symmetry at the transition lines. The FLP-F is an insulator-metal transition, whereas the CAF-PLP is an insulator-insulator transition. The resulting qualitative dependence of the edge transport gap $\Delta_{\rm edge}$ is plotted in Fig 3.

Canted antiferromagnetic phase. We now identify the insulating $\nu=0$ phase observed in Refs. [4, 6] at electric energy $\epsilon_V < \epsilon_V^*$ below the critical value $\epsilon_V^* \approx E^* a_z/2 \approx 20 B_\perp[\mathrm{T]K}$. The F phase at $\epsilon_V < \epsilon_V^*$ is ruled out as having metallic $2e^2/h$ edge conductance. The phase at high enough $\epsilon_V \gtrsim \epsilon_V^*$ is readily identified as the FLP phase and hence it cannot also occur at lower electric field. The PLP phase at $\epsilon_V < \epsilon_V^*$ (ILC at $\epsilon_V = 0$) is ruled out, since the transition between the PLP and FLP phases is continuous and the system would be insulating at all ϵ_V values. The phase at $\epsilon_V < \epsilon_V^*$ is therefore the remaining

insulating CAF phase of the $\nu=0$ QHFM. The evolution of the system with applied electric field is denoted by a violet line in Fig. 3. The conductance spike at $\epsilon_V=\epsilon_V^*$ thus corresponds to the CAF-PLP insulator-insulator transition, which is the only such transition on the phase diagram (Figs. 2 and 3); upon further increasing the electric field, the PLP phase continuously transitions to the FLP phase, with the system remaining insulating at $\epsilon_V>\epsilon_V^*$.

The conclusion about the CAF phase implies that the isospin anisotropy (2) favors the AF phase, i.e., that in real BLG the case

$$u_z > -u_{\perp} > 0 \tag{5}$$

is realized. This is consistent with microscopic considerations. In BLG, the leading anisotropy $u_z>0$ arises from e-e interactions due to a finite layer separation. This "capacitance effect" favors equal charge population of the layers and the anisotropy energy $\mathcal{E}_{\diamond}(P)$ with only $u_z>0$ present is minimized by the states $\chi_a=|K\rangle\otimes|\mathbf{s}_a\rangle$, $\chi_b=|K'\rangle\otimes|\mathbf{s}_b\rangle$ with arbitrary spin polarizations $\mathbf{s}_{a,b}$ of the layers (it can also be demonstrated [21] that at this level these are, in fact, exact eigenstates at any layer separation, which suggests their particular robustness). This spin degeneracy is then lifted by the competition between the anisotropy u_\perp and the Zeeman effect. The negative $u_\perp<0$ favoring antiferromagnetic order can naturally arise from e-ph or renormalized e-e interactions [12, 13, 27].

The critical electric energy ϵ_V^* is related to $u_{\perp,z}$ and ϵ_Z according to Eq. (4) for the CAF-PLP transition. Given the large discrepancy between ϵ_V^* and $\epsilon_Z \approx 0.7 B[T] K$ at moderate tilt angles, one may neglect ϵ_Z to obtain

$$\epsilon_V^* = \sqrt{u_z^2 - u_\perp^2}. (6)$$

At smaller $|u_\perp|$, ϵ_V^* is mainly determined by u_z : at $|u_\perp| \lesssim u_z/2$, one may also neglect $|u_\perp|$ with decent accuracy to extract the anisotropy $u_z \approx \epsilon_V^* \approx 20 B_\perp [{\rm T}] {\rm K}$. The magnitude and linear B_\perp -dependence of ϵ_V^* at higher $B_\perp \gtrsim 2 {\rm T}$ in Ref. [4] are fully consistent with the properties of the bare anisotropies $u_{\perp,z}^{(0)}(B_\perp)$, whereas the deviation from linearity at lower $B_\perp \lesssim 2 {\rm T}$ can be explained by enhanced renormalizations of $u_{\perp,z}(B_\perp)$ as the transition to the low-magnetic-field interaction-induced state of debated nature [28–32] is approached.

Tilted-field experiment. Tilting the magnetic field by a moderate 45° angle $(B/B_{\perp} = \sqrt{2})$ in Ref. [4] resulted in a small yet systematic increase of the critical ϵ_V^* value, which is also consistent with Fig. 3 and Eq. (4), but did not induce any new phase transitions. However, according to the phase diagram in Fig. 3, upon further increasing the tilt ratio B/B_{\perp} , the CAF-F and FLP-F transitions will eventually occur. The tilt ratio $B/B_{\perp} = 2|u_{\perp}|/(\mu_B B_{\perp})$ required for reaching the F phase is determined by the value of $|u_{\perp}|$, which cannot

be obtained from ϵ_V^* [Eq. (6)] independently of u_z and for smaller $|u_\perp| \lesssim u_z/2$ remains essentially unknown. The most favorable case would be $|u_\perp| \ll u_z$. For reference, at "large" $|u_\perp| = u_z/2 \approx 10 B_\perp$ [T]K, the required tilt ratio is $B/B_\perp \approx 30$. Since the low-electric-field insulating $\nu=0$ state is detectable at as low as $B_\perp \approx 1$ T [4–6], the practical tilt ratio as high as $B/B_\perp \sim 50$ could be achieved in BLG for available static magnetic fields $B \leq 45$ T.

Outlook. Provided the F phase can be reached by tilting the magnetic field, it becomes possible to explore the whole phase diagram (Fig. 3) of the $\nu=0$ QHFM in dualgated BLG devices. The predicted marked distinction between the edge transport properties of the "spin-active" CAF and spin-singlet FLP phases – gradual closing of the edge gap $\Delta_{\rm edge}$ with tilting the field vs its insensitivity – should manifest itself in such an experiment as continuous CAF-F vs sharp FLP-F insulator-metal transitions. These features can also be used to test the presented theory and distinguish between the phases in the experiment.

Author is thankful to P. Coleman for insightful discussions and helpful comments on the manuscript and to E. Andrei, C. N. Lau, A. Young, and M. Foster for insightful discussions. The work was supported by the U.S. DOE Grants No. DE-FG02-99ER45790 and No. DE-AC02-06CH11357.

- J. G. Checkelsky, Lu Li, and N. P. Ong, Phys. Rev. Lett.
 100, 206801 (2008); Xu Du, I. Skachko, F. Duerr, A. Luican, and E. Y. Andrei, Nature 462, 192 (2009); K. I. Bolotin, F. Ghahari, M. D. Shulman, H. L. Stormer, and P. Kim, Nature 462, 196 (2009).
- [2] B. E. Feldman, J. Martin, and A. Yacoby, Nature Phys. 5, 889 (2009).
- [3] Y. Zhao, P. Cadden-Zimansky, Z. Jiang, and P. Kim, Phys. Rev. Lett. 104, 066801 (2010).
- [4] R. T. Weitz, M. T. Allen, B. E. Feldman, J. Martin, and A. Yacoby, Science 330, 812 (2010).
- [5] F. Freitag, J. Trbovic, M. Weiss, and C. Schönenberger, Phys. Rev. Lett. 108, 076602 (2012).
- [6] J. Velasco, Jr., L. Jing, W. Bao, Y. Lee, P. Kratz, V. Aji, M. Bockrath, C. N. Lau, C. Varma, R. Stillwell, D. Smirnov, Fan Zhang, J. Jung, and A. H. MacDonald, Nature Nanotech. 7, 156 (2012).
- [7] S. M. Girvin and A. H. MacDonald, in *Perspectives in Quantum Hall Effects*, edited by S. Das Sarma and A. Pinczuk (John Wiley and Sons, New York, 1997).
- [8] K. Nomura and A. H. MacDonald, Phys. Rev. Lett. 96, 256602 (2006).
- [9] K. Yang, S. Das Sarma, and A. H. MacDonald, Phys. Rev. B 74, 075423 (2006).
- J. Alicea and M. P. A. Fisher, Phys. Rev. B 74, 075422 (2006); M.O. Goerbig, R. Moessner, and B. Doucot, Phys. Rev. B 74, 161407 (2006).
- [11] J. Jung and A.H. MacDonald, Phys. Rev. B 80, 235417 (2009).

- [12] K. Nomura, S. Ryu, and D.-H. Lee, Phys. Rev. Lett. 103, 216801 (2009); C.-Yu Hou, C. Chamon, and C. Mudry, Phys. Rev. B 81, 075427 (2010).
- [13] M. Kharitonov, Phys. Rev. B 85, 155439 (2012).
- [14] Y. Barlas, R. Cote, K. Nomura, and A. H. MacDonald, Phys. Rev. Lett. 101, 097601 (2008).
- [15] D. A. Abanin, S. A. Parameswaran, and S. L. Sondhi, Phys. Rev. Lett. 103, 076802 (2009).
- [16] E. V. Gorbar, V. P. Gusynin, and V. A. Miransky, Phys. Rev. B 81, 155451 (2010).
- [17] R. Nandkishore and L. Levitov, arXiv:1002.1966 (2010).
- [18] D. A. Abanin, P. A. Lee, and L. S. Levitov, Phys. Rev. Lett. 96, 176803 (2006).
- [19] H.A. Fertig and L. Brey, Phys. Rev. Lett. 97, 116805 (2006).
- [20] V. P. Gusynin, V. A. Miransky, S. G. Sharapov, and I. A. Shovkovy, Phys. Rev. B 77, 205409 (2008).
- [21] M. Kharitonov (to be published).
- [22] E. McCann and V. Falko, Phys. Rev. Lett. 96, 086805 (2006).
- [23] Note that E is indeed the field created by the gates, while the "self-action" layer charge imbalance effects are systematically taken into account by the anisotropy (2).

- [24] Note that quantum fluctuations do not diverge in the infrared in 2+1=3 space-time dimensions and are therefore not essential for QHFM systems.
- [25] V. Mazo, E. Shimshoni, and H. A. Fertig, Phys. Rev. B 84, 045405 (2011).
- [26] Due to strong screening [16], bulk and edge transport gaps in BLG scale as $\hbar^2/(ml_B^2)$ (*m* is the effective mass).
- [27] The CAF phase due to a different microscopic mechanism (superexchange) was predicted to exist in semiconductor QH bilayers at $\nu=2$ in S. Das Sarma, S. Sachdev, and L. Zheng, Phys. Rev. Lett. **79**, 917 (1997); Phys. Rev. B **58**, 4672 (1998).
- [28] E. V. Castro, N. M. R. Peres, T. Stauber, and N. A. P. Silva, Phys. Rev. Lett. 100, 186803 (2008).
- [29] R. Nandkishore and L. Levitov, Phys. Rev. Lett. 104, 156803 (2010); Phys. Rev. B 82, 115124 (2010).
- [30] F. Zhang, H. Min, M. Polini, and A. H. MacDonald, Phys. Rev. B 81, 041402 (2010).
- [31] O. Vafek and K. Yang, Phys. Rev. B 81, 041401 (2010).
- [32] Y. Lemonik, I. L. Aleiner, C. Toke, and V. I. Falko, Phys. Rev. B 82, 201408 (2010).